

## DETERMINATION OF SHEAR WAVE VELOCITIES AND DENSITIES FROM *P*-WAVE AMPLITUDES IN VSP DATA<sup>1</sup>

S. CHENG<sup>2</sup>, F. HRON<sup>3</sup> AND P.F. DALEY<sup>3</sup>

### ABSTRACT

In the amplitude inversion of seismic data any uncertainty in the source wavelet, source radiation characteristic or imperfect coupling between the ground and individual geophones have large detrimental effects on the inversion results. In this paper we show how the impact of these difficulties may be minimized if we apply a standard iterative procedure, based on Singular Value Decomposition (SVD), to the ratio of vertical components of primary downgoing and upgoing longitudinal waves recorded using vertical seismic profiling (VSP) techniques. As this paper is to be regarded as a feasibility study exploring the potential of the method, it has been applied to noise-free synthetic data in a horizontally layered medium composed of perfectly elastic layers whose thicknesses are larger than the predominant wavelength.

We employed a "layer stripping method" to recover the shear wave velocity and the volume mass density in a given layer during a single computer run. In this manner, we achieved a very fast convergence rate, usually requiring less than seven iterations, and a high degree of numerical accuracy in the inversion of synthetic data. It should be mentioned that because of the general validity of the basic equations (1) and (2), which may be applied to any one-dimensional structure with no thin-layered transition zones, the proposed method can be employed in an inversion process involving such geological structures. The method is currently being applied to real data by the first-named author in the People's Republic of China.

### INTRODUCTION

Generalized linear inverse theory has been used extensively in various areas of geophysics where inversion problems occur. In seismology Aki and Lee (1976), Crosson (1976), Neumann (1981), Benz and Smith (1984), Hirahara and Ishikawa (1984), Ivansson (1985) and Chiu et al. (1986) employed this method to invert traveltime data recorded on the surface of the earth. It has also been applied to the inversion of vertical seismic profiles (VSP) traveltime data (McMechan, 1983; Lines et al., 1984; Stewart, 1984; Pujol et al., 1985). Additionally, several attempts to invert amplitude

data recorded at the earth's surface have been made (Shahriar et al., 1987) in an effort to obtain elastic parameters of a subsurface geological model in terms of the (compressional) *P*-wave velocities ( $\alpha$ ), (shear) *S*-wave velocities ( $\beta$ ) and volume mass densities ( $\rho$ ).

In this paper we deal with the amplitude inversion of unconverted primary *P*-waves of multioffset VSP data. The Singular Value Decomposition (SVD) technique (Aki and Richards, 1980; Lines and Treitel, 1984) is used in the inversion algorithm, while the parameterization of the forward problem is based on Asymptotic Ray Theory (ART) (Hron, 1968; Červený and Ravindra, 1971; Hron and Kanasevich, 1971). The ratios of the vertical displacements of upgoing waves (reflected waves) to downgoing waves (transmitted waves) are used as the observation data in the inversion algorithm. We employ displacement ratios, rather than individual displacements, to avoid a rather troublesome initial amplitude problem.

The initial amplitude at the source is difficult to estimate. This difficulty may be avoided if the ratio of the displacements of two different rays, propagating from the source to the receiver along very similar raypaths, is used as input into the inversion algorithm rather than the particle displacement of a single ray. Two such rays, radiated from the source, *S*, with almost identical amplitudes are shown in Figure 1. They both reach the geophone, *G*, in the borehole as primary downgoing and upgoing unconverted *P*-waves. Such waves can be identified in the VSP seismograms and their signatures will also be utilized in the determination of the shear wave velocities and volume mass densities of the individual layers, in addition to the compressional wave velocities and layer thicknesses, which are traditionally recovered from this type of data.

The use of displacement ratios of the primary downgoing and upgoing waves in the inversion process has some practical advantages. The adverse effects of unpredictable factors, such as random inhomogeneities in the medium, local

<sup>1</sup>Presented at the C.S.E.G. National Convention, Calgary, Alberta, May 16, 1990. Manuscript received by the Editor April 20, 1991; revised manuscript received October 17, 1991.

<sup>2</sup>Permanent address: Southwest Petroleum Institute, Nanchong, Sichuan, People's Republic of China

<sup>3</sup>Department of Physics, University of Alberta, Edmonton, Alberta T6G 2J1

This research project was supported by a Natural Sciences and Engineering Research Council of Canada (NSERC) operating grant, 0009157. It was carried out during a one-year working visit of S. Cheng at the Department of Physics, University of Alberta, under the existing cultural exchange agreement between the People's Republic of China and Canada. The authors wish to express their appreciation for the constructive comments of the reviewers which have enhanced the clarity of the text.

variations in the curvature of geological interfaces and imperfect coupling between the ground and the geophone, are considerably suppressed. This becomes obvious if we realize that the two rays, which are recognized at the receiver as being the primary downgoing and upgoing waves, travel in close proximity through the same part of the medium between the source and the geophone. As a consequence, both are similarly influenced by the geological and structural unconformities encountered along their raypaths.

General techniques for the separation of upgoing and downgoing waves are not discussed here, as they are described at length in the literature pertaining to this subject (Lee and Balch, 1983; Seeman and Horowicz, 1983). For the same reason, the major features of VSP techniques are not dealt with here, as references on this topic may be found in numerous papers and monographs, for example, the book by Galperin (1974). Instead, we will concentrate on the main advantages of the presented inversion approach by exploring its theoretical foundations and practical imitations and by presenting numerical examples.

**FORWARD MODEL COMPUTATION**

Computation of the seismic response of an interim geological model at some given stage of the iterative inversion process (the so-called forward-problem solution) plays an important role in any inversion technique based on an iterative approach. Understandably, the forward-modelling method should be fast yet sufficiently accurate to make the inversion as efficient as possible in terms of the CPU time employed for the inversion. Preferably, it should be based on a theory that can be applied to a wide variety of geological models and requires minimal adjustments for any special features which may be encountered. For this reason we have selected Asymptotic Ray Theory (ART) as the basis for the ray amplitude computation in our computer program. This method has been successfully employed in the past in the computation of ray based synthetic seismograms for complex geological structures, which in general consist of inhomogeneous layers separated by curved interfaces (Hron, 1973; May and Hron, 1978) and featuring varying degrees of anelasticity (Krebs and Hron, 1980) or anisotropy (Daley and Hron, 1979). The most recent modifications to ART, which include a more accurate treatment in the vicinity of critical points (Marks and Hron, 1979) and caustics (Choi and Hron, 1981) have been used in the computation of the synthetic traces.

For the requirements of this paper we will present only formulae for the zero-order approximation of ART, in which the amplitude of each ray is represented by the first term in an infinite asymptotic series (Hron, 1968; Červený and Ravindra, 1971; Hron and Kanasewich, 1971). In this approximation the longitudinal component of particle motion, that is, the component along the direction of the ray, for any unconverted *P*-wave propagating from the source, *S*, to the geophone, *G*, along a raypath passing through *J* points of the incidence (*O*<sub>1</sub>, *O*<sub>2</sub>, . . . , *O*<sub>*J*</sub>) in a horizontally layered medium (Figure 2) is given as a function of time by

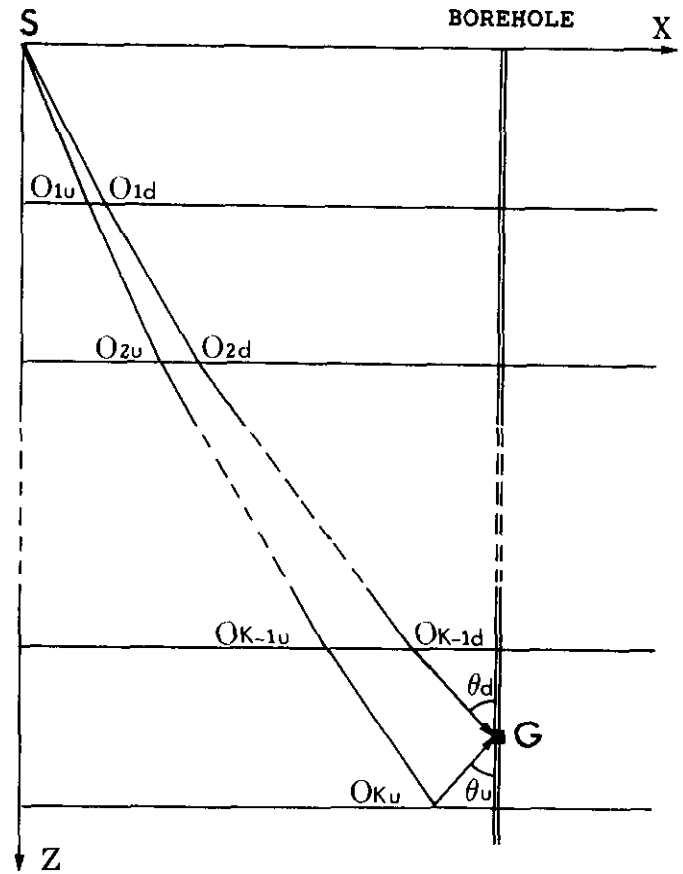


Fig. 1. Geometry of raypaths of the primary downgoing (subscript "d") and upgoing (subscript "u") rays from the surface source, *S*, to the geophone, *G*, which is buried on the vertical profile in the *K*th layer of the horizontally layered medium.

$$u_G(t) = \frac{A_o(\theta_o)}{L} \left[ \frac{z_o^-}{z_o^+} \right]^{\frac{1}{2}} \left[ \prod_{j=1}^J \left[ \frac{z_j^-}{z_j^+} \right]^{\frac{1}{2}} R_j \right] f[t - \tau_G] \tag{1}$$

Here the following notation has been used:

- f*(*t*) – the time dependence of the source pulse;
- $\tau_G$  – the arrival time of the disturbance (pulse) at the geophone, *G*;
- A*<sub>o</sub>( $\theta_o$ ) – the initial ray amplitude expressed as a function of the take-off angle,  $\theta_o$ , of the ray at the source;
- L* – the geometrical spreading (spherical divergence) along the ray tube;
- R*<sub>*j*</sub> – the reflection or transmission coefficient at the *j*th point of incidence, *O*<sub>*j*</sub> (*j* = 1, 2, . . . , *J*);
- z*<sub>*j*</sub><sup>+</sup> – the wave impedance, which is equal to the product of the wave speed and the volume mass density of the wave incident at *O*<sub>*j*</sub>;
- z*<sub>*j*</sub><sup>-</sup> – the wave impedance at the same point, *O*<sub>*j*</sub>, but related to the reflected or transmitted wave;

$z_0$  and  $z_G$  – the impedances at the source and the geophone, respectively.

The absolute value of the geometrical spreading,  $L$ , in any horizontally layered medium, with no lateral inhomogeneities, is equal to (Hron, 1968; Červený and Ravindra, 1971; Hron and Kanasevich, 1971):

$$L = \left| x_G \frac{\partial x_G}{\partial \theta} \frac{\cos \theta_G}{\sin \theta_0} \right|^{\frac{1}{2}} \prod_{j=1}^J \left[ \frac{\cos \theta_j^+}{\cos \theta_j^-} \right]^{\frac{1}{2}}, \quad (2)$$

where the individual symbols have the following meanings (see Figure 2):

- $x_G$  – the horizontal distance from the source to the geophone;
- $\theta_j^+$  and  $\theta_j^-$  – the angle of incidence and the angle of reflection or transmission at the  $j$ th point of incidence,  $O_j$ , respectively;
- $\theta_0$  and  $\theta_G$  – the acute angles between the ray and the vertical axis at the source,  $S$ , and the geophone,  $G$ , respectively.

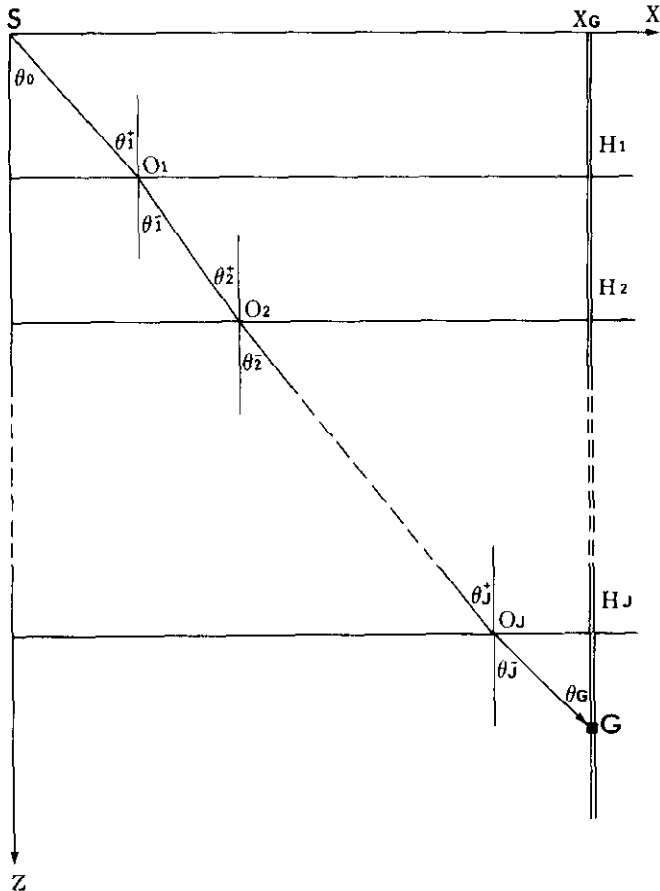


Fig. 2. Introduction of the symbols needed for the ray amplitude expressions given by equations (1), (2), (7) and (8) in the text. Note that the thickness of the  $j$ th layer ( $j = 1, 2, \dots, J$ ) is given by  $h_j = H_j - H_{j+1}$ , where  $H_j$  is the depth from the surface to the bottom of the  $j$ th layer.

It should be noted that the above expressions for the displacement [equation (1)] and the geometrical spreading [equation (2)] are valid for any horizontally layered medium with an arbitrary velocity-depth structure. This is also true for the plane wave reflection and transmission coefficients, whose values depend on the velocity and density contrasts across an interface, and the angle of incidence.

In special circumstances, such as in the case of plane, homogenous horizontal layers considered in this paper, the formulae for the particle displacement and the geometrical spreading may be simplified considerably if one realizes that the assumption of homogeneity implies that the wave impedances at the top and bottom of the same layer are identical, or in our notation (Figure 2):

$$z_j^- = z_{j+1}^+, \quad (j = 1, 2, \dots, J-1) \quad (3)$$

and

$$z_0 = z_1^+, \quad z_G = z_J^-.$$

Assumed homogeneity within a layer also means that the individual ray segments are straight, thereby making the same angle with the vertical at both ends of a given ray segment, so that

$$\theta_j^- = \theta_{j+1}^+, \quad (j = 1, 2, \dots, J-1) \quad (4)$$

and

$$\theta_0 = \theta_1^+, \quad \theta_G = \theta_J^-.$$

In this way, the displacement relation, equation (1), may be rewritten with the help of equation (3) as

$$W_G(t) = \frac{A_0(\theta_0)}{L} \prod_{j=1}^J R_j f(\xi), \quad (5)$$

where  $\xi = t - \tau_G$  is the phase of the wavelet. The geometrical spreading,  $L$ , originally given by equation (2) may also be expressed in accordance with equation (4) as

$$L = \left| x_G \frac{\partial x_G}{\partial \theta} \frac{\cos \theta_G}{\sin \theta_0} \right|^{\frac{1}{2}}. \quad (6)$$

The standard explicit formulae for the reflection and transmission coefficients,  $R_j$ , may be found in Červený and Ravindra (1971).

It follows from equation (5) that the particle motion of the wave depends on two distinct parameters of the source, namely:

- (a) its radiation pattern characterized by  $A_0(\theta_0)$ , representing the initial amplitude of the ray leaving the source with an angle of  $\theta_0$ , and
- (b)  $f(t)$ , which describes the shape of the source wavelet for all rays in the time domain.

It should be noted that whereas  $f(t)$  remains the same for all of the rays radiated from the source,  $A_O(\theta_O)$  is usually some smoothly varying function of  $\theta_O$  for realistic sources, creating a special pattern which becomes a unique characteristic of the source that is very difficult to reconstruct from real data. It is for these reasons that there is a motivation to eliminate both  $A_O(\theta_O)$  and  $f(t)$  from any inversion process involving real data.

Intuitively, we feel that the above objective may be accomplished by using a ratio of particle displacements of two neighboring rays, as it is well-known that the radiation characteristic,  $A_O(\theta_O)$ , for a highly concentrated explosive source is usually a slowly varying function of the take-off angle  $\theta_O$ .

If we utilize equations (5) and (6) for two primary rays as displayed in Figure (1) and labelled as upgoing (subscript "u") and downgoing (subscript "d"), the ratio of their maximum vertical displacements (displacements amplitudes)  $\chi$  becomes

$$\chi = \frac{(-\cos\theta_{Gu})}{(+\cos\theta_{Gd})} \frac{L_d \prod_{j=1}^K R_{ju}}{L_u \prod_{j=1}^{K-1} R_{jd}} = \frac{R_{Ku} \prod_{j=1}^{K-1} R_{ju} / R_{jd}}{-\tilde{L}} \quad (7)$$

where

$$\tilde{L} = \left| \frac{+\cos\theta_{Gd} L_u}{-\cos\theta_{Gu} L_d} \right| = \frac{\cos\theta_{Gd}}{\cos\theta_{Gu}} \left| \frac{\sum_{j=1}^{K+1} (h_j v_j) / \cos^3 \theta_{ju}^+}{\sum_{j=1}^K (h_j v_j) / \cos^3 \theta_{jd}^+} \right|^{1/2} \quad (8)$$

The notation, which has been used in the above equations, may be found in Figure 1 where both raypaths are schematically displayed.

It is seen in that figure that the raypath for the downgoing primary P-wave reaches the geophone, G, located in the Kth layer after passing through (K-1) points of the incidence  $O_{jd}$  ( $j = 1, 2, \dots, K-1$ ). In contrast, the upgoing raypath passes through K points of incidence  $O_{ju}$  ( $j = 1, 2, \dots, K$ ). The relevant reflection or transmission coefficient at the jth point of incidence for the downgoing and upgoing rays are denoted as  $R_{jd} = R(O_{jd})$  and  $R_{ju} = R(O_{ju})$ , respectively.

It should be noted that the ratio of the cosines of the angles of incidence of both waves are required in equation (7) to convert the longitudinal components of particle motion of both waves into the vertical components, which are registered at the geophone, G.

The reflection and transmission coefficients  $R_j$  together with the partial derivatives  $\partial R/\partial \rho$ ,  $\partial R/\partial \beta$  and  $\partial R/\partial \alpha$ , which are also required in the inversion process, are real quantities in the precritical range of offsets considered in this paper. It is their sign that determines the polarity of the vertical particle motion registered at the geophone. The positive or negative value of the reflection coefficients is directly related to

the ratio of the impedances on both sides of the interface at a given point of incidence  $O_j$ . This sign must be preserved in the input data in order to obtain correct results as is done to obtain the values in Figure 6.

On the other hand, the product of the ratios of the geometrical spreadings and the cosines of the angles of incidence never change sign in the type of medium considered in this paper, making it possible to consider only their absolute value denoted by  $\tilde{\tau}$  in equation (8).

### INVERSION METHOD

Our inversion process, applied to the ratio of the vertical displacements of the related upgoing and downgoing waves registered at the same geophone within a borehole, is based on the Singular Value Decomposition method. Since there are several excellent tutorial texts on the subject (Aki and Richards, 1980; Lines and Treitel, 1984; Lines and Levin, 1988) together with the availability of relevant software in this area (Lawson and Hanson, 1974), we will restrict ourselves to the presentation of a brief overview of the basic concepts and formulae of this method and refer the reader seeking a more detailed discussion to the above literature.

We achieve linearization of our general inverse problem by expanding the vertical displacement ratio  $\chi$ , which according to equation (7) is a generally inhomogeneous function of  $m$  model parameters ( $p_1, p_2, \dots, p_m$ ) in a Taylor series expansion, and retaining only its first two terms:

$$\chi = \chi^O + \sum_{j=1}^m \frac{\partial \chi}{\partial p_j} \Big|_{p_i=p_i^O} (p_j - p_j^O) \quad (9)$$

In the above formulae,  $\chi^O$  is the computed ratio related to the initial set of model parameters  $p_j^O$  ( $j = 1, 2, \dots, m$ ), whereas  $\chi$  is the known observed response due to the still unknown parameters  $p_j$ .

If, for a given model represented by the same set of  $m$  parameters  $p_j$  ( $j = 1, 2, \dots, m$ ) there are  $n$  observed values of  $\chi_i$  ( $i = 1, 2, \dots, n$ ),  $n \geq m$ , the set of unknown model parameters may be formally obtained by solving a system of  $n$  linear algebraic equations for the  $m$  unknown model parameters. This may be conveniently written in matrix notation as

$$\mathbf{q} = \mathbf{Gd} \quad (10)$$

Here,

$$\mathbf{q} = (\chi_1 - \chi_1^O, \chi_2 - \chi_2^O, \dots, \chi_n - \chi_n^O)^T \quad (11)$$

is what is known as the discrepancy vector, and

$$\mathbf{d} = (p_1 - p_1^O, p_2 - p_2^O, \dots, p_m - p_m^O)^T \quad (12)$$

is called the model perturbation vector. The superscript "T" denotes the transpose. The matrix  $\mathbf{G}$ , given by

$$\mathbf{G} = \left\| \frac{\partial \chi_i}{\partial p_j} \right\| \quad (i = 1, 2, \dots, n), (j = 1, 2, \dots, m), \quad (13)$$

is an  $n \times m$  Jacobian matrix of partial derivatives.

Since the actual inverse problem is nonlinear, the linearized equation (9) must be solved iteratively. For a relatively small number of model parameters,  $m$ , represented in our case by the seismic velocities  $\alpha$ ,  $\beta$ , the mass density  $\rho$ , and the thickness  $h$  in each of the layers, the Singular Value Decomposition technique is generally considered to be very efficient (Lines and Treitel, 1984; Nolet, 1987).

In this technique, the matrix  $\mathbf{G}$  in equation (10) is factored into the product of three matrices as

$$\mathbf{G} = \mathbf{U}\mathbf{\Lambda}\mathbf{V}^T, \quad (14)$$

so that in each iteration step the components of the model perturbation vector [equation (12)] may be recovered by applying the inverse operator,

$$\mathbf{G}^{-1} = \mathbf{V}\mathbf{\Lambda}^{-1}\mathbf{U}^T, \quad (15)$$

to the current value of the discrepancy vector  $\mathbf{q}$  in equation (11), as given in the following relation:

$$\mathbf{d} = \mathbf{V}\mathbf{\Lambda}^{-1}\mathbf{U}^T\mathbf{q}. \quad (16)$$

The three individual matrices in equation (14) have, according to the theory of Singular Value Decomposition (Lines and Treitel, 1984), the following meanings:

$\mathbf{U}$  is the matrix whose columns are composed of the eigenvectors  $\mathbf{u}$ . Each eigenvector corresponds to the nonzero eigenvalue,  $\lambda^2$ , which is the solution of the eigenvalue problem,

$$\mathbf{G}\mathbf{G}^T\mathbf{u} = \lambda^2\mathbf{u}; \quad (17)$$

$\mathbf{V}$  is the matrix with column vectors corresponding to the eigenvectors  $\mathbf{v}$  of the problem,

$$\mathbf{G}^T\mathbf{G}\mathbf{v} = \lambda^2\mathbf{v}; \text{ and} \quad (18)$$

$\mathbf{\Lambda}$  is a diagonal matrix whose elements are the positive square roots of the eigenvalues  $\lambda^2$  of  $\mathbf{G}^T\mathbf{G}$  in equation (18), i.e.,

$$\Lambda_{ii} = +|\lambda_i|.$$

Several computer programs for Singular Value Decomposition are available, together with a discussion of the pertinent mathematical background (Forsythe et al., 1977; Longley, 1984). They may be readily used in any iterative process such as that implied by equation (16).

The iterative process is terminated when the components of the model perturbation vector are smaller than some

predetermined values, thereby indicating that the last set of computed model parameters  $p_j$  ( $j = 1, 2, \dots, m$ ) produces  $n$  computed values  $\chi_i^O$  ( $i = 1, 2, \dots, n$ ) which approach the  $n$  observed values  $\chi_i$  within an acceptable accuracy. The final set of model parameters is then declared to be the result of the inversion process and computation is terminated.

## DISCUSSION OF NUMERICAL RESULTS

Results of several numerical experiments will be presented in this section. We emphasize that these numerical experiments were designed to test the feasibility of our approach in extracting shear wave velocities and volume mass densities of a layered medium from the vertical components of particle motion of unconverted  $P$ -waves recorded in a borehole employing the vertical seismic profiling (VSP) method. Hence, the inversion was tested with noise-free synthetic data obtained with the help of our computer programs for the numerical simulation of the seismic response of horizontally layered geological structures.

These programs, which are based on the ray approach and thereby are suitable for the computation of displacement ratios needed in our inversion process, have been thoroughly tested by comparing their results with those produced by the so-called full-wave methods (Hron et al., 1974). The programs are briefly described in another paper, Hron et al., 1986, where they were employed in the computation of seismic records for various types of horizontally layered structures frequently encountered in oil exploration.

Our numerical experiments showed that the correct shear wave velocity and volume mass density in each layer could be obtained with very few iterations, which never exceeded seven regardless of the initial values, provided that they were within geologically acceptable limits. This efficiency and high degree of accuracy was achieved by what has been termed the "layer stripping method". The merits of this method have been discussed in an earlier paper (Shahriar et al., 1987). There it was demonstrated that one could minimize the propagation of numerical noise while still maintaining a high degree of resolution if the number of model parameters used in the inversion process during an individual computer run was small. In our experience, it has been found that it is preferable to keep the number of model parameters less than five.

Thus during each computer run we utilized the vertical displacement ratio  $\chi$  [equation (7)] of the upgoing and downgoing unconverted  $P$ -waves to recover the shear wave velocity,  $\beta_{(K+1)}$ , and the volume mass density,  $\rho_{(K+1)}$ . Medium  $(K+1)$  underlies medium  $K$  in which the geophone is located (Figure 1).

In this manner, we restricted the number of model parameters being simultaneously inverted to two. This number is equal to the quantity  $m$  in equation (12), where all other model parameters needed in equation (7) were assumed to be known or had been determined in a previous stage of the inversion process. For example, in the four-layer model

described in Table I, the thicknesses  $h_j$ , densities  $\rho_j$ , and shear wave velocities  $\beta_j$  in all three overlying layers ( $j = 1, 2, 3$ ), together with the  $P$ -wave velocities  $\alpha_j$  ( $j = 1, 2, 3, 4$ ) in each of the four upper layers had to be known before we could determine the shear wave velocity and volume mass density in the fourth layer. After five iterations these values were found to be  $\beta_4 = 2.89$  km/s and  $\rho_4 = 2.15$  g/cm<sup>3</sup>, regardless of the initial values of  $\beta_4^0$  and  $\rho_4^0$ , as Tables IV and V testify.

The input data for this particular run consisted of six numerical values of the vertical displacement ratios  $\chi_n$  ( $n = 1, 2, \dots, 6$ ) obtained for geophone  $G_3$  buried at the depth of 0.9 km in the third layer, at six different offsets ranging from 0.3 km to 1.3 km at increments of 0.2 km (see Figure 3). The numerical values of the set of six  $\chi_n$  may be inferred from the curve  $G_3$  in Figure 6. This curve is based on the corresponding curves  $G_3$  in Figures 4 and 5, where the dependence of the vertical displacement on the offset for upgoing and downgoing waves is shown.

Prior to that, the traveltimes were used to establish the  $P$ -wave velocities  $\alpha_j$  and thicknesses  $h_j$  ( $j = 1, 2, 3, 4$ ) following the method described in Shahriar et al. (1987). The traveltimes curves for the reflected (upgoing) primary waves, which were used for this purpose, are shown in Figure 7 with Table II giving the details of the inversion. As these preliminary procedures are well-documented in the above paper, no further discussion of this rather straightforward process will be provided here.

It should be pointed out that the  $P$ -wave velocity  $\alpha_5$  in the half-space in our four-layered model (Table I) had to be recovered from the ratios of the vertical displacements  $\chi_n$  obtained from the fourth geophone location,  $G_4$ , in the fourth layer at the depth of 1.20 km as shown in Figure 3. The six ratios pertaining to the six offsets displayed in Figure 3 were computed from curves  $G_4$  in Figures 4 and 5. They were utilized as the input data for a single run in which the other two model parameters, the shear wave velocity  $\beta_5$  and density  $\rho_5$  of the half-space were also determined simultaneously in seven iterations, as indicated in Table III.

This modification of our program for the simultaneous determination of all three model parameters in the half-space ( $\alpha_5$ ,  $\beta_5$  and  $\rho_5$ ) was done mainly to demonstrate its versatility, where a different number of model parameters may be obtained from the same input data.

Additionally, this diversion also confirms that the efficiency of the method of computation, indicated by the number of iterations, decreases with the number of model parameters that are being simultaneously inverted. This is seen graphically by comparing Table III with Tables IV and V. It also explains the reason we have chosen to determine the compressional velocities  $\alpha_j$  and the layer thicknesses  $h_j$  ( $j = 1, \dots, 4$ ) from the reflected traveltimes. This had the effect of reducing the number of parameters which had to be obtained from the displacement ratios to two per run; the shear wave velocities  $\beta_j$  and the volume mass densities  $\rho_j$  ( $j = 1, \dots, 4$ ).

In tables IV, V, VI and VII, where the results of our standard (unknown shear wave velocities and volume mass den-

Layer	$\alpha$ (km/s)	$\beta$ (km/s)	$\rho$ (g/cm <sup>3</sup> )	$h$ (km)
1	4.00	2.31	1.77	0.50
2	4.40	2.54	1.92	0.20
3	4.20	2.43	1.84	0.30
4	5.00	2.89	2.15	0.40
5	5.50	3.18	2.34	half-space

**Table I.** Parameters for a four-layered model over a half-space with  $\alpha_j$ ,  $\beta_j$ ,  $\rho_j$  and  $h_j$  denoting the longitudinal wave velocity, the shear wave velocity, the volume mass density and the thickness of the  $j$ th layer, respectively. This model was used for the computation of the synthetic data employed in the inversion technique.

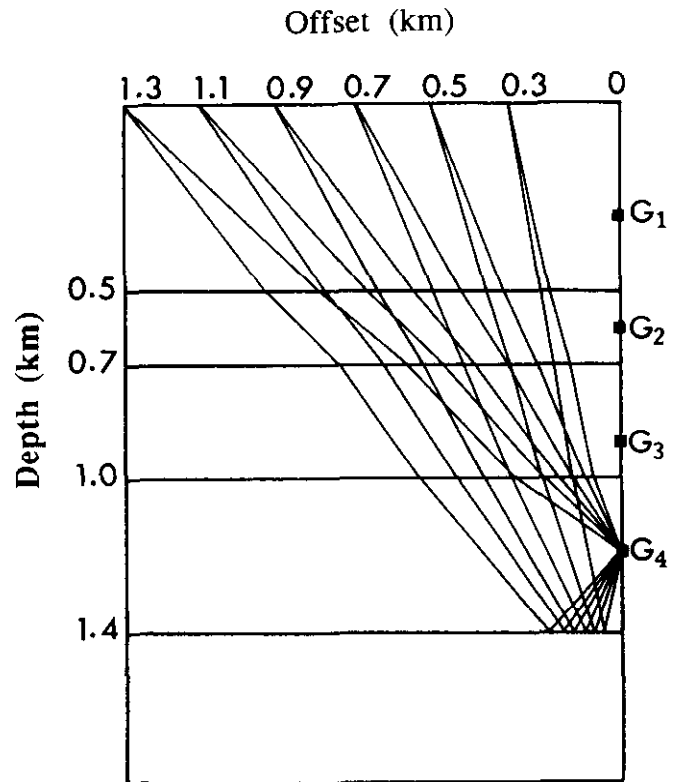


**Fig. 3.** Geometry of the raypaths, whose traveltimes and amplitudes were used in the inversion, for a four-layered model given in Table I. The 6 offsets ranged from 0.3 km to 1.3 km at 0.2 km increments. The depths of the four geophone locations were 0.3 km, 0.6 km, 0.9 km and 1.2 km, respectively.

sities) inversion of VSP data is displayed, the values of the model parameters for the surface layer are not listed. The reason for this is that appropriate values may be determined directly from surface measurements, assuming homogeneity in that layer.

After having presented an overview of our inversion strategy of VSP data, a detailed examination of the efficiency and accuracy of the results displayed in Tables IV to VII is

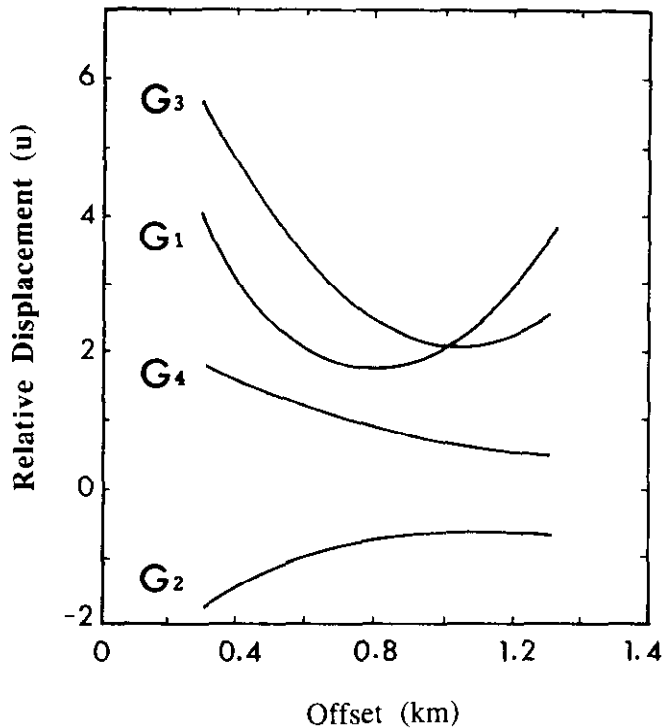


Fig. 4. Relative vertical displacements of the upgoing (reflected) rays computed for the model in Table I according to equations (5) and (6). The four different geophone locations, which were used in labelling the curves, are given in Figure 3. Note that the negative values for the  $G_2$  curve are due to the negative values of the reflection coefficient obtained for the bottom of the second layer.

straightforward and does not require many additional comments. It should be mentioned that in our case of noise-free data, the correct shear wave velocity and volume mass density were always obtained to within four digits of accuracy in no more than five iterations, regardless of the initial estimates, as illustrated in Tables IV and V.

A separate numerical experiment, in which we investigated the influence on the inversion results by some incorrectly specified initial values of the shear wave velocity and the volume mass density in the surface layer, was also conducted. Specifically, we knowingly contaminated the correct values  $\beta_1$  and  $\rho_1$  of Table I, which represent the actual values of the shear wave velocity and the volume mass density in the surface layer. The contamination consisted of specifying one of the two quantities mentioned above with a relative error of approximately 10 percent, when compared to their correct values. The inversion process was then invoked with both the actual and contaminated data initial values as input, and the effect on how this influenced the recovery of the other model parameters in the lower layers was examined. In practice, such a situation is not uncommon if the surface layer is not truly homogenous or if errors in the measurements of the shear wave velocity,  $\beta_1$ , or the volume mass density,  $\rho_1$ , occur.

Results of computer runs related to this experimentation are displayed in Table VI (for a 9.96 percent relative error in

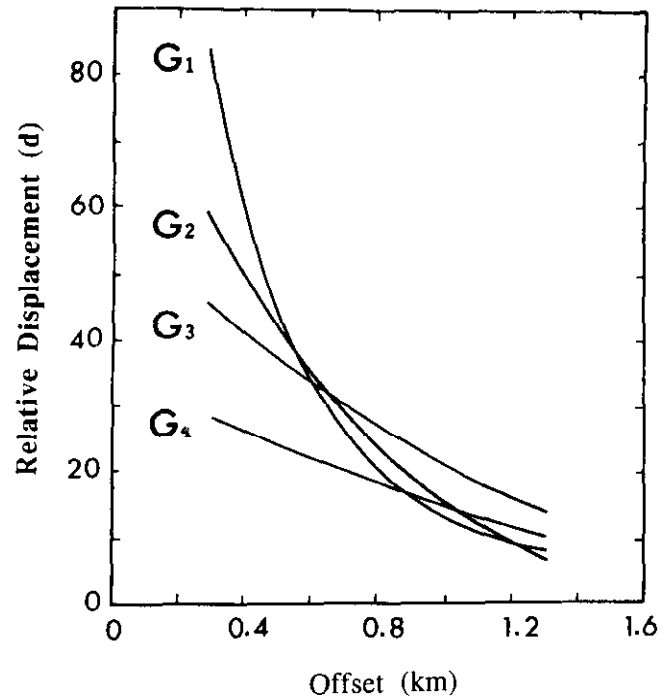


Fig. 5. Relative vertical displacement of the downgoing (transmitted) rays computed for the model in Table I according to equations (5) and (6). The four different geophone locations are given in Figure 3.

$\beta_1$ ) and Table VII (for a 10.17 percent relative error in  $\rho_1$ ). One can easily infer from Table VI that the initial error in  $\beta_1$  hampers the recovery of the correct values for the shear wave velocities, while the accuracy in the determination of the volume mass densities remains almost unchanged. On the other hand, the contents of Table VII demonstrates that an incorrect value of  $\rho_1$  by 10.17 percent permanently distorts the volume mass densities in subsequent stages of the inversion process.

Fortunately, as indicated by the results in Table VII, the inverted velocities, which in most cases are the primary objective of any inversion process, are virtually immune to errors in density determination and, as a consequence, we need not be unduly concerned by them.

## CONCLUSIONS

In this paper we have provided a detailed discussion of both the theoretical and numerical aspects of our newly proposed method designed for the simultaneous extraction of shear wave velocities and mass densities from the amplitude ratios of the vertical components of compressional ( $P$ ) waves recorded by the VSP technique.

This type of input is required for the determination of the shear wave velocity and volume mass density from the unconverted  $P$ -wave data, since it is the amplitude of compressional waves which is explicitly influenced by these parameters.

Inversion of the amplitude ratios of the vertical components was carried out during an iterative process based on the Singular Value Decomposition method. The ray amplitude

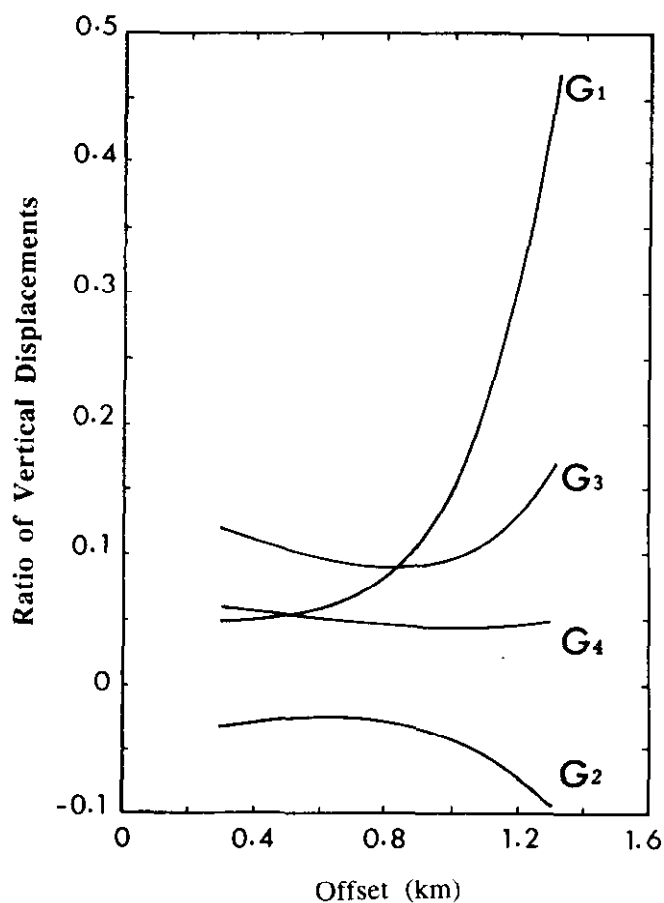


**Fig. 6.** Ratios of vertical displacements of the upgoing and downgoing rays for the four different geophone locations given in Figure 3. The ratios, computed from the curves in Figures 4 and 5, were used as input for our iterative inversion procedure. We used a layer stripping approach, in which the shear wave velocity,  $\beta_{j+1}$ , and the volume mass density,  $\rho_{j+1}$ , were determined during a single run utilizing 6 values on each of the  $G_j$  curves ( $j = 1, 2, 3, 4$ ) as the input. The results of the inversion are given in Tables III through VII. They are also discussed in detail in the text.

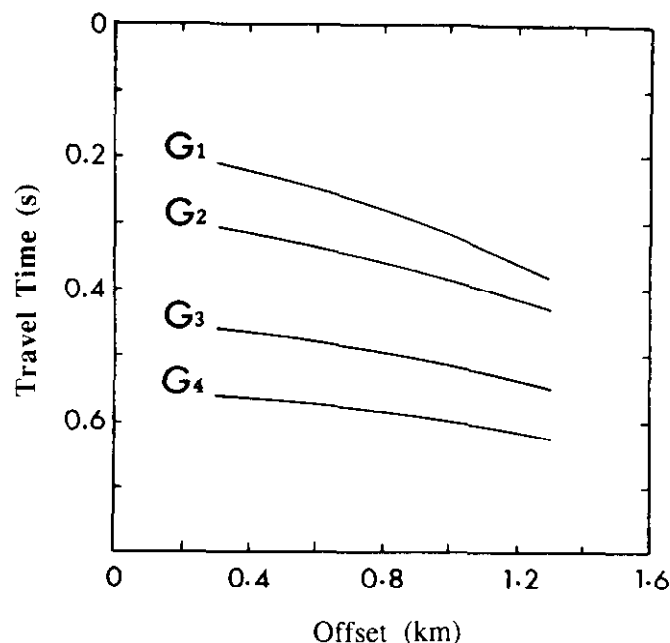


**Fig. 7.** The traveltimes curves for the reflected (upgoing) rays computed for the model in Table I and the four different geophone locations shown in Figure 3. Six values of each curve,  $G_j$ , were used as input for the simultaneous determination of the longitudinal wave velocity,  $\alpha_j$ , and the layer thickness,  $h_j$ , ( $j = 1, 2, 3, 4$ ). The results of our layer stripping inversion approach are tabulated in Table II.

computation in the forward numerical modelling was performed using Asymptotic Ray Theory. The rapid convergence was achieved by employing a layer stripping approach, in which inversion proceeds from the top to the bottom of the model. Hence, only two parameters of the model, namely, the shear wave velocity and the volume mass density within a given layer, were to be determined in a single computer run.

As the research described in this paper has been part of a wider study exploring fundamental theoretical and numerical aspects of the proposed method which would determine the feasibility of its application to real data, we have used

Layer	$\alpha$ (km/s)			h(km)			Number of iterations
	initial	inverted	exact	initial	inverted	exact	
1	3.6000	4.0000	4.0000	0.8000	0.5000	0.5000	3
2	3.6000	4.4000	4.4000	0.8000	0.2000	0.2000	4
3	3.6000	4.2000	4.2000	0.8000	0.3000	0.3000	4
4	3.6000	5.0000	5.0000	0.8000	0.4000	0.4000	4

**Table II.** Results of our layer stripping inversion process during which the longitudinal wave velocity,  $\alpha_j$ , and the thickness,  $h_j$ , were obtained for the  $j$ th layer ( $j = 1, 2, 3, 4$ ), utilizing 6 values from the curve  $G_j$  in Figure 7 as input. These values represent traveltimes of the upgoing (reflected) waves arriving at the geophone  $G_j$  located in the  $j$ th layer (see Figure 3).



noise-free synthetic data to represent the seismic response of a horizontally layered medium composed of homogeneous layers, whose thicknesses were larger than the predominant wavelength.

We showed that regardless of the starting values of the linearized inversion process (subject only to general geological and geophysical constraints) the correct values of seismic shear wave velocities and volume mass densities were recovered in less than seven iterations for noise-free data. We have

	initial	inverted	exact	Number of iterations
$\alpha_5$ (km/s)	3.6000	5.5000	5.5000	
$\beta_5$ (km/s)	2.4000	3.1800	3.1800	7
$\rho_5$ (g/cm <sup>3</sup> )	2.0000	2.3400	2.3400	

**Table III.** Results of the simultaneous determination of the longitudinal wave velocity,  $\alpha_5$ , the shear wave velocity,  $\beta_5$ , and the volume mass density,  $\rho_5$ , for the half-space. They were obtained in 7 iterations in a single computer run using 6 different vertical displacement ratios of the downgoing and upgoing waves registered at geophone  $G_4$  located at a depth of 1.2 km in the fourth layer, as shown in Figure 3.

noticed that our technique provides a healing process when recovering the seismic velocities after a deliberate introduction of error in the shear wave velocity,  $\beta_1$ , in the surface layer. No such healing in the determination of the volume mass densities has been observed when the volume mass density,  $\rho_1$ , was contaminated.

In principle, our method can be applied to any one-dimensional model composed of thick layers with an arbitrary velocity structure, as our basic formulae (1) and (2) are valid for any horizontally layered medium with no thinly layered transition zones.

The greatest advantage of our method, namely its independence of the actual shape of the source wavelet and its associated radiation pattern, together with its insensitivity to local structural unconformities and nonuniform coupling between the individual geophones and the ground, is now being tested on the interpretation of real data carried out by the first-named author at the Southwest Petroleum Institute, Nanchong, Sichuan, People's Republic of China.

REFERENCES

Aki, K. and Lee, W.H.K., 1976. Determination of three-dimensional velocity anomalies under a seismic array using first *P* arrival times from local earthquakes: *J. Geophys. Res.* **81**, 4381-4399.

Layer	$\beta$ (km/s)			$\rho$ (g/cm <sup>3</sup> )			Number of iterations
	initial	inverted	exact	initial	inverted	exact	
2	2.4000	2.5400	2.5400	2.0000	1.9200	1.9200	4
3	2.4000	2.4300	2.4300	2.0000	1.8400	1.8400	5
4	2.4000	2.8900	2.8900	2.0000	2.1500	2.1500	5
5	2.4000	3.1800	3.1800	2.0000	2.3400	2.3400	4

**Table IV.** The first set of results of our layer stripping inversion process in which the shear wave velocities,  $\beta_j$ , and the volume mass densities,  $\rho_j$  ( $j = 2, 3, 4, 5$ ) were determined simultaneously from 6 vertical displacement ratios in a single computer run. The 6 input values of the vertical displacement ratios were taken from curve  $G_1$  in Figure 6. Note that the surface layer values of  $\beta_1 = 2.31$  km/s and  $\rho_1 = 1.77$  g/cm<sup>3</sup>, which are needed for the inversion, were supposedly correctly obtained from independent surface measurements.

Layer	$\beta$ (km/s)			$\rho$ (g/cm <sup>3</sup> )			Number of iterations
	initial	inverted	exact	initial	inverted	exact	
2	3.2000	2.5400	2.5400	3.0000	1.9200	1.9200	4
3	3.2000	2.4300	2.4300	3.0000	1.8400	1.8400	5
4	3.2000	2.8900	2.8900	3.0000	2.1500	2.1500	5
5	3.2000	3.1800	3.1800	3.0000	2.3400	2.3400	4

**Table V.** The second set of results of the same layer stripping inversion process obtained for the same input data as in Table IV but with different initial values.

Layer	$\beta$ (km/s)			$\rho$ (g/cm <sup>3</sup> )		
	inverted	exact	relative error (%)	inverted	exact	relative error (%)
2	2.7346	2.5400	7.66	1.9206	1.9200	0.03
3	2.6411	2.4300	8.69	1.8407	1.8400	0.04
4	3.0437	2.8900	5.32	2.1534	2.1500	0.15
5	3.3087	3.1800	4.05	2.3441	2.3400	0.17

**Table VI.** Results of our layer stripping process for the same input data and initial data as in Table IV, but with a different surface layer value of the shear wave velocity  $\beta_1 = 2.54$  km/s. Note that the 9.96 % relative error in  $\beta_1$  has influenced the accuracy of the inversion process.

Layer	$\beta$ (km/s)			$\rho$ (g/cm <sup>3</sup> )		
	inverted	exact	relative error (%)	inverted	exact	relative error (%)
2	2.5400	2.5400	0.00	2.1152	1.9200	10.17
3	2.4300	2.4300	0.00	2.0271	1.8400	10.17
4	2.8900	2.8900	0.00	2.3686	2.1500	10.17
5	3.1800	3.1800	0.00	2.5780	2.3400	10.17

**Table VII.** Results of our layer stripping process for the same input data and initial data as in Table IV, but with a different surface layer value of the volume mass density  $\rho_1 = 1.95$  g/cm<sup>3</sup>. Note that the 10.17% relative error in  $\rho_1$  has significantly influenced the accuracy of the mass density determination but has left the accuracy in determining the shear wave velocity unchanged.

\_\_\_\_\_ and Richards, P., 1980, Quantitative Seismology, Vol. 2: W.H. Freeman & Co.

Benz, H.M. and Smith, R.B., 1984, Simultaneous inversion for lateral velocity variations and hypocenter in the Yellowstone region using earthquake and refraction data: *J. Geophys. Res.* **89**, 1208-1220.

Červený, V. and Ravindra, R., 1971, Theory of seismic head waves: Univ. of Toronto Press.

Chiu, S.K.L., Kanasewich, E.R. and Phadke, S., 1986, Three-dimensional determination of structure and velocity by seismic tomography: *Geophysics* **51**, 1559-1571.

Choi, A.P. and Hron, F., 1981, Amplitude and phase shift due to caustics: *Bull. Seis. Soc. Am.* **71**, 1445-1461.

Crosson, R.S., 1976, Crustal structure modelling of earthquake data, 1. Simultaneous least squares estimation of hypocenter and velocity parameters: *J. Geophys. Res.* **81**, 3036-3046.

Daley, P.F. and Hron, F., 1979, *SH* waves in a layered transversely isotropic media – an asymptotic expansion approach: *Bull. Seis. Soc. Am.* **69**, 689-711.

Forsythe, G.E., Malcolm, M.A. and Moler, C.B., 1977, Computer methods for mathematical computations: Prentice Hall, Inc.

Gaiperin, E.I., 1974, Vertical seismic profiling: *Soc. Expl. Geophys.*

Hirahara, K. and Ishikawa, Y., 1984, Travel time inversion for three dimensional *P*-wave velocity anisotropy: *J. Phys. Earth* **32**, 197-218.

Hron, F., 1968, Introduction to the ray theory in a broader sense: application to seismology, in *Textbook of laboratoire de physique de l'école normale supérieure: Univ. de Paris.*

\_\_\_\_\_, 1973, A numerical ray generation and its application to the computation of synthetic seismograms for complex layered media: *Geophys. J.* **35**, 345-349.

\_\_\_\_\_ and Kanasewich, E.R., 1971, Synthetic seismograms for deep seismic sounding studies using asymptotic ray theory: *Bull. Seis. Soc. Am.* **61**, 1169-1200.

\_\_\_\_\_, \_\_\_\_\_ and Alpaslan, T., 1974, Partial ray expansion required to suitably simulate the exact wave solution: *Geophys. J.* **36**, 607-625.

\_\_\_\_\_, May, B.T., Covey, J.D. and Daley, P.F., 1986, Synthetic seismic sections for acoustic, elastic, anisotropic and vertically inhomogeneous layered media: *Geophysics* **51**, 710-735.

Ivansson, S., 1985, A study of methods for tomographic velocity estimation in the presence of low-velocity zones: *Geophysics* **50**, 969-988.

Krebes, E.S. and Hron, F., 1980, Ray synthetic seismograms for *SH* waves in anelastic media: *Bull. Seis. Soc. Am.* **70**, 29-46.

Lawson, C.L. and Hanson, R.J., 1974, Solving least squares problems: Prentice Hall, Inc.

Lec, M.W. and Balch, A.H., 1983, Computer processing of vertical seismic profile data: *Geophysics* **48**, 272-287.

Lines, L.R. and Levin, F.K., 1988, Inversion of geophysical data: *Soc. Expl. Geophys.*

\_\_\_\_\_, and Treitel, S., 1984, Tutorial – a review of least-squares inversion and its application to geophysical problems: *Geophys. Prosp.* **32**, 159-186.

\_\_\_\_\_, Bourgeois, A. and Covey, J.D., 1984, Travelttime inversion of offset vertical seismic profiles – a feasibility study: *Geophysics* **49**, 250-264.

Longley, J.W., 1984, Least square computations using orthogonalization methods: Marcel Dekker.

Marks, L.W. and Hron, F., 1979, Dynamic properties of reflected and head waves near the critical points: *Can. J. Earth Sci.* **16**, 1388-1401.

May, B.T. and Hron, F., 1978, Synthetic seismic sections of typical petroleum traps: *Geophysics* **43**, 1119-1147.

## DETERMINATION OF SHEAR WAVE VELOCITIES AND DENSITIES

- McMechan, G.A., 1983, Seismic tomography in boreholes: *Geophys. J. Roy. Astr. Soc.* **74**, 601-612.
- Neumann, G., 1981, Determination of lateral inhomogeneities in reflection seismics by inversion of travel time residuals: *Geophys. Prosp.* **29**, 161-177.
- Nolet, G., 1987, Seismic wave propagation and seismic tomography, *in* Nolet, G., Ed., *Seismic tomography*: Reidel Publ. Co.
- Pujol, J., Burridge, R. and Smithson, S., 1985, Velocity determination from offset vertical seismic profiling data: *J. Geophys. Res.* **90**, 1871-1880.
- Seeman, B. and Horowicz, L., 1983, Vertical seismic profiling: separation of upgoing and downgoing acoustic waves in a stratified medium: *Geophysics* **48**, 555-568.
- Shahriar, M., Hron, F. and Cumming, G.L., 1987, Linearized inversion of seismic amplitude data: *J. Can. Soc. Expl. Geophys.* **23**, 56-65.
- Stewart, R.R., 1984, VSP interval velocities from travel time inversion: *Geophys. Prosp.* **32**, 608-628.